Instrumental Odour Monitoring System Optimized for Drone Applications

Javier Alonso-Valdesueiro*†, Santiago Marco-Colás*† and Agustín Gutiérrez-Gálvez*†
* Department of Electronic and Biomedical Engineering, University of Barcelona,
† Signal and Information Processing for Sensing Systems, Institute for Bioengineering of Catalunya

***Abstract*—In this contribution, a novel design for an Instrumental Odour Monitoring System (IOMS) is presented. This evolution of the IOMS concept is designed to be mounted on a drone, enabling the generation of 3D maps of gas concentrations and odour levels during flight. It features fast-response gas chambers, a rapid data acquisition architecture, a modular design, and fast GPS RTK tracking. The performance of this innovative design has been tested under controlled conditions, comparing its performance with existing designs. The results show that the time for the gas concentration inside the IOMS to reach the limit of detection of the sensors is approximately 3-7 seconds faster than that observed in traditional IOMS designs. Additionally, measurements taken during test flights with a conventional IOMS are compared with those obtained using the new design. In every flight, the new IOMS produces results tenths of seconds faster than the conventional designs. These results, both in the laboratory and in the field, indicate that the modifications in the new IOMS design enable it to respond rapidly to changes caused by the drone's swift movements. This fast response and rapid tracking make the novel design more suitable for fast 3D map of gas concentrations and odour levelthan conventional IOMS designs.**

***Index Terms*—IOMS; Drone-based odour monitoring; 3D odour mapping; Gas concentration mapping; Fast-response gas chambers; Electronic nose; Malodours; Machine learning; Odour intensity prediction**

I. Introduction

INSTRUMENTAL Odour Monitoring Systems (IOMS) have been deployed in Wastewater Treatment Plants (WWTPs) over the past decade [1]–[4]. These systems are used for odour quantification and monitoring due to their effectiveness in measuring gases such as H_2S, NH_3, and others producing malodorous [5], [6]. Consequently, in recent years, they have become commercial products and are being installed at WWTP fences and critical points across Europe [4], [7]–[9]. However, these deployments are time-consuming, requiring extensive and costly calibration procedures. Furthermore, they lack flexibility in case of plant changes and cannot produce a comprehensive map of the plant unless multiple IOMS units are deployed around and inside the facility [10].

In recent years, drone-based IOMS have emerged for rapid gas concentration characterization and odour mapping in the industrial landscape [11]–[13]. Their applications include methane leak control [14], fire detection with source location [15], and air quality monitoring [16]. In particular, studies on WWTPs have shown that these systems can produce 3D maps of gas concentration results much faster than commercial IOMS for the entire plant [17], enabling data scientists to develop odour quantification models [18], [19].

Despite these results, experience has shown that drone-mounted designs struggle to follow rapid variations of its surrounding air [12], [13], [19]. Consequently, the drone's speed (typically $\sim$10 $^{m}/_{s}$) when moving around the plant for 3D mapping is limited by the response time of the measuring system. Also, windy conditions produce plumes of odour and the conventional IOMSs struggle to work in these conditions (wind speed ≤ 10 $^{km}/_{h}$). This limitation reduces the applicability of IOMSs to quantify static sources and operate in favorable conditions.

Recent studies have shown that a careful design of the gas chambers containing the sensors in an IOMS significantly reduces the time needed to reach the sensors' limit of detection [20]. This reduction in response time impacts on the requirements of sensor data and GPS location data acquisition architectures of the IOMS. Consequently, the traditional IOMS design, even in its drone-mounted version [12], requires a substantial review.

This work presents the mentioned review of the conventional IOMS design, featuring a very fast response time, rapid data acquisition architecture, and centimeter-precise RTK GPS location. This platform is capable of tracking rapid changes in the surrounding air, addressing the limitations of conventional IOMSs when mounted on drones (such as drone speed and windy weather conditions). During laboratory tests, the novel design has shown faster response (in the tenths of seconds) to an odorous step than a conventional IOMS and fast plume tracking. This behavior has been confirmed during test flights (at UPC facilities droneLab, Castelldefels, Spain).

Therefore, this contribution is organized as follows: Section II provides a description of the novel IOMS, including its gas chambers, data acquisition architecture, communications, and GPS data management. Section III presents a comprehensive performance characterization of the IOMS by comparing its response in various experiments with that of a conventional design. Section IV summarizes the flying tests assessing the IOMS performance. Finally, Section V summarizes the achievements of this design, outlining the potential applications of this optimized IOMS.

This contribution has been funded from ATTRACT, a European Union Horizon 2020 research and innovation project, under grant agreement No. 101004462. The research has been also partially funded by IBEC-CERCA consortium and Generalitat de Catalunya (expedient 2021 SGR 01393).
Manuscript received April 19, 2021; revised August 16, 2021.

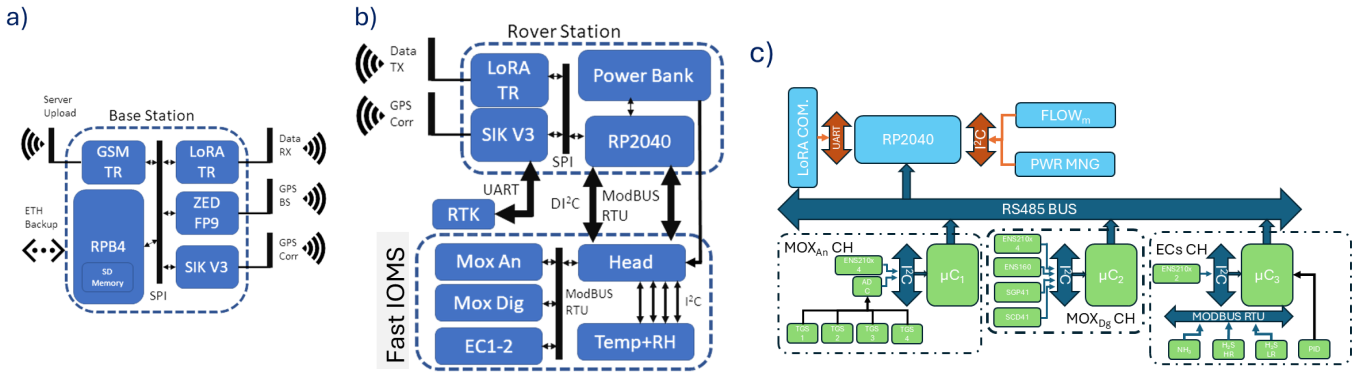

Fig. 1: Graphical description of the Instrumental Odour Monitoring System. a) Block diagram of the Base Station (BS). It is based on a Raspberry pi 4B+ and communicates with the mobile part of the IOMS via Peer two Peer LoRA connection. It also provide GPS data to the RTK GPS module for corrections and communicates with an external server via GSM router. b) Block diagram of the mobile part of the IOMS. The Rover Station (RS) is placed on the drone and it controls the power consumption and gets data from the FastIOMS system. This system provides data from three chambers, each with different sensors inside, air flow coming inside the the chambers and temperature and relative humidity of the air in contact with each sensor.

II. IOMS Description

Figures 1 (a), (b) and (c) show the architecture of the novel IOMS. The system is divided in two parts. The mobile part contains the Rover Station (RS), ther RTK GPS system, and the Fast IOMS (see figure 2). The ground based system (Base Station or BS) is placed near by the fliying area for monitoring, logging and control duties.

The RS is placed on the drone and it controls the power consumption and gets data from the FastIOMS system. This system provides data from three chambers, each with different sensors inside, air flow coming inside the the chambers and temperature and relative humidity of the air in contact with each sensor. This data is sent via Peer-to-Peer LoRA communication to the BS. At BS, the data is plotted for information of the operator, logged in a hardrive and sent to an external server for further analysis. The BS connects with the external serve via a GSM router.

At the same time the data from the Fast-IOMS is logged data with centimeter precission is added to the generated files. This data is provided by the RTK GPS module once the module recives GPS location from the BS and makes its corrections. The module is based on a ZED-F9P module from U-Blox.

Fig. 2: Novel IOMS mounted on the drone with the Bag Sampler. The Rover Station is placed close to the drone chassis for protection. The Fast IOMS and Bag Sampler air inlets are connected two both 10 meters PTFE tubes.

A. Fast IOMS

The Fast-IOMS consists of 4 chambers with 3 electrochemical sensors, one Photo Ionization Detector (PID), and MOx sensors from different manufacturers. Table 1 summarizes the sensors placed inside the chambers. Every chamber has its own microcontroller (μC) SAMD21 for acquiring and transmitting the data. Each has a hardware interrupt line that activates the communication protocol via RS485. The μCs also have a USB-C port for debugging and stand-alone functionality.

The MoxAn chamber consists of 4 small cavities (0.6 cm^3) accommodating 4 TGS MOx sensors from Figaro. Currently, the sensors (TGS2600, TGS2602, TGS2611, and TGS2620) operate with the same PWM signal applied to their heater resistance. Voltage is acquired using an ADS1115 ADC connected to the μC via I^{2}C. Table I summarizes the sensors placed inside each chamber.

Temperature and relative humidity inside each cavity are sampled by ENS210 sensors from Sensirion. The resistance of the 4 MOx sensors is sent to the RS via RS485 at a maximum rate of 10 Hz, along with the data from the ENS210 sensors, sampled every second. With a similar design, the MoxDig chamber consists of 4 small cavities where 3 digital MOx sensors and one photoacoustic sensor are placed. The SGP41, the ENS160, and the BM688 are configured in their single-shot acquisition mode. The SCD41 is configured in its periodic sampling mode. As in the MoxAn chamber, 4

TABLE I: Summary of the sensors placed inside each chamber and their main characteristics.

Chamber	**Chamber Characteristics**		
	Sensors Included	*Chamber Volume* (cm^3)	*Number of ENS*210 (°, *RH*(%))
MoxAn	TGS2600, TGS2602, TGS2611, TGS2620	0.6	4
MoxDig	SGP41, ENS160, BM688, SCD41	0.6	4
ECS	H2S/C-50, H2S/C-200	4	1
ECs+PID	NH3/C-100, PID	4	1

ENS210 sensors are placed inside for temperature and relative humidity monitoring.

The other two chambers host 3 electrochemical sensors from Membrapor and a Photoionization Detector (PID) from Alphasense. The H_2S sensors are placed together in the same chamber with an additional ENS210 sensor monitoring temperature and relative humidity inside. The NH_3 sensor is placed in the second chamber with the PID, also with an additional ENS210 sensor. The electrochemical sensors are controlled by a PCB from Membrapor and the voltage produced by the PID is acquired using an ADS1115 ADC.

The raw data from the three are sent to the RS at a maximum rate of 1 $^{Hz}/_{sensor}$ along with their corresponding temperature and relative humidity data from the ENS210 sensors (sampled every 6 seconds).

The Fast-IOMS also hosts a pump connected upstream of the fluidic path. It can provide 3.5 slm of air mass flow when every chamber is connected to it. A flow meter (FS2012 from Renesas) has been placed at the entrance of the chambers to monitor the air entering the Fast-IOMS. This data is sent directly to the RS via differential I2C.

B. Rover Station

As it is shown in figure 2, the RS is comfortably attached to the lower belly of the AAurelia X8 octocopter. Ther RS is based on a two core RP2040 μC which controls the power consumption of the Flying system (Fast-IOMS and itself) via I^2C. It si connected to the Fast-IMS via a RS485 bus (as depicted in figure 1 (c)) and produces bursts of data every 2 seconds. Each burst of data corresponds to one chamber and contains 6 different measurments of every sensor stamped with the corresping temperature and Relative humidity data.

Each data burst is packed and set to the BS via Peer-to-Peer LoRA communication. The LoRA module is controlled via a Serial-UART bus (see figure 1 (c)).

III. IOMS Performance Characterization

http://www.latex-community.org/
https://tex.stackexchange.com/

IV. Drone-mounted IOMS and Flight Performance

See [**?**], [**?**], [**?**], [**?**], [**?**] for resources on formatting math into text and additional help in working with LaTeX.

V. Conclusions

For some of the remainer of this sample we will use dummy text to fill out paragraphs rather than use live text that may violate a copyright.

Itam, que ipiti sum dem velit la sum et dionet quatibus apitet voloritet audam, qui aliciant voloreicid quaspe volorem ut maximusandit faccum conemporerum aut ellatur, nobis arcimus. Fugit odi ut pliquia incitium latum que cusapere perit molupta eaquaeria quod ut optatem poreiur? Quiaerr ovitior suntiant litio bearciur?

Onseque sequaes rectur autate minullore nusae nestiberum, sum voluptatio. Et ratem sequiam quaspername nos rem repudandae volum consequis nos eium aut as molupta tectum ulparumquam ut maximillesti consequas quas inctia cum volectinusa porrum unt eius cusaest exeritatur? Nias es enist fugit pa vollum reium essusam nist et pa aceaqui quo elibusdandis deligendus que nullaci lloreri bla que sa coreriam explacc atiumquos simolorpore, non prehendunt lam que occum [**?**] si aut aut maximus eliaeruntia dia sequiamenime natem sendae ipidemp orehend uciisi omnienetus most verum, ommolendi omnimus, est, veni aut ipsa volendelist mo conserum volores estisciis recessi nveles ut poressitatur sitiis ex endi diti volum dolupta aut aut odi as eatquo cullabo remquis toreptum et des accus dolende pores sequas dolores tinust quas expel moditae ne sum quiatis nis endipie nihilis etum fugiae audi dia quiasit quibus. Ibus el et quatemo luptatque doluptaest et pe volent rem ipidusa eribus utem venimolorae dera qui acea quam etur aceruptat. Gias anis doluptaspic tem et aliquis alique inctiuntiur?

Sedigent, si aligend elibuscid ut et ium volo tem eictore pellore ritatus ut ut ullatus in con con pere nos ab ium di tem aliqui od magnit repta volectur suntio. Nam isquiante doluptis essit, ut eos suntionsecto debitiur sum ea ipitiis adipit, oditiore, a doloreremposaut harum ius, atquat.

Rum rem ditinti sciendunti volupiciendi sequiae nonsect oreniatur, volores sition ressimil inus solut ea volum harumqui to see(1) mint aut quat eos explis ad quodi debis deliqui aspel earcius.

$$x = \sum_{i=0}^{n} 2iQ. \tag{1}$$

Alis nime volorempera perferi sitio denim repudae pre ducilit atatet volecte ssimillorae dolore, ut pel ipsa nonsequiam in re nus maiost et que dolor sunt eturita tibusanis eatent a aut et dio blaudit reptibu scipitem liquia consequodi od unto ipsae. Et enitia vel et experferum quiat harum sa net faccae dolut voloria nem. Bus ut labo. Ita eum repraer rovitia samendit aut et volupta tecupti busant omni quiae porro que nossimodic temquis anto blacita conse nis am, que ereperum eumquam quaescil imenisci quae magnimos recus ilibeaque cum etum iliate prae parumquatemo blaceaquiam quundia dit apienditem rerit re eici quaes eos sinvers pelecabo. Namendignis as exerupit aut magnim ium illabor roratecte plic tem res apiscipsam et vernat untur a deliquaest que non cus eat ea dolupiducim fugiam volum hil ius dolo eaquis sitis

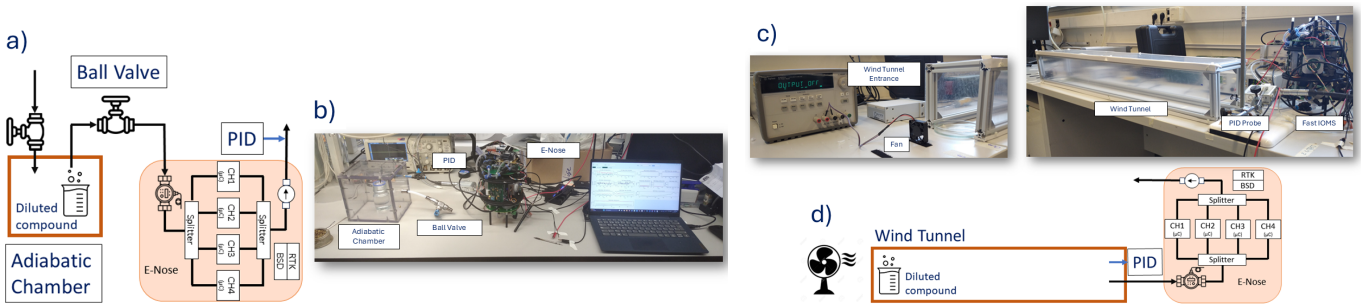

Fig. 3: Experimental setups used for characterizing the Fast IOMS system at the laboratory. a) First setup: the fast IOMS is connected to ball valve acting as a exhaust valve of an adiabatic chamber. The diluted compound is placed inside the chamber and leaved there for 5 minutes with the inlet valve and the exhaust valve closed. After 5 minutes both valves are open and the Fast IOMS inlet is connected to the exhaust valve for data logging. b) Practical realization of the first experimental setup. c) Second setup: The Fast IOMS inlet is placed alongside the probe tip of a 201B miniPID from AURORA Inc. at the end of a wind tunnel. At the entrance of the wind tunnel, a small petri dish with 25mL of the diluted compound with a small fan is placed. The fan is turned on and off in 20 seconds intervals. d) Practical realization of the second setup.

aut landesto quo corerest et auditaquas ditae voloribus, qui optaspis exero cusa am, ut plibus.

VI. Some Common Elements

A. Sections and Subsections

Enumeration of section headings is desirable, but not required. When numbered, please be consistent throughout the article, that is, all headings and all levels of section headings in the article should be enumerated. Primary headings are designated with Roman numerals, secondary with capital letters, tertiary with Arabic numbers; and quaternary with lowercase letters. Reference and Acknowledgment headings are unlike all other section headings in text. They are never enumerated. They are simply primary headings without labels, regardless of whether the other headings in the article are enumerated.

B. Citations to the Bibliography

The coding for the citations is made with the LaTeX `\cite` command. This will display as: see [**?**].

For multiple citations code as follows: `\cite{ref1,ref2,ref3}` which will produce [**?**], [**?**], [**?**]. For reference ranges that are not consecutive code as `\cite{ref1,ref2,ref3,ref9}` which will produce [**?**], [**?**], [**?**], [**?**]

C. Lists

In this section, we will consider three types of lists: simple unnumbered, numbered, and bulleted. There have been many options added to IEEEtran to enhance the creation of lists. If your lists are more complex than those shown below, please refer to the original "IEEEtran_HOWTO.pdf" for additional options.

A plain unnumbered list:

bare_jrnl.tex
bare_conf.tex
bare_jrnl_compsoc.tex
bare_conf_compsoc.tex
bare_jrnl_comsoc.tex

Fig. 4: Simulation results for the network.

A simple numbered list:

1) bare_jrnl.tex
2) bare_conf.tex
3) bare_jrnl_compsoc.tex
4) bare_conf_compsoc.tex
5) bare_jrnl_comsoc.tex

A simple bulleted list:

- bare_jrnl.tex
- bare_conf.tex
- bare_jrnl_compsoc.tex
- bare_conf_compsoc.tex
- bare_jrnl_comsoc.tex

D. Figures

Fig. 1 is an example of a floating figure using the graphicx package. Note that `\label` must occur AFTER (or within) `\caption`. For figures, `\caption` should occur after the `\includegraphics`.

Fig. 2(a) and 2(b) is an example of a double column floating figure using two subfigures. (The subfig.sty package must be loaded for this to work.) The subfigure `\label` commands

(a) (b)

Fig. 5: Dae. Ad quatur autat ut porepel itemoles dolor autem fuga. Bus quia con nessunti as remo di quatus non perum que nimus. (a) Case I. (b) Case II.

TABLE II: An Example of a Table

One	Two
Three	Four

are set within each subfloat command, and the `\label` for the overall figure must come after `\caption`. `\hfil` is used as a separator to get equal spacing. The combined width of all the parts of the figure should do not exceed the text width or a line break will occur.

Note that often IEEE papers with multi-part figures do not place the labels within the image itself (using the optional argument to `\subfloat[]`), but instead will reference/describe all of them (a), (b), etc., within the main caption. Be aware that for subfig.sty to generate the (a), (b), etc., subfigure labels, the optional argument to `\subfloat` must be present. If a subcaption is not desired, leave its contents blank, e.g.,`\subfloat[]`.

VII. Tables

Note that, for IEEE-style tables, the `\caption` command should come BEFORE the table. Table captions use title case. Articles (a, an, the), coordinating conjunctions (and, but, for, or, nor), and most short prepositions are lowercase unless they are the first or last word. Table text will default to `\footnotesize` as the IEEE normally uses this smaller font for tables. The `\label` must come after `\caption` as always.

VIII. Algorithms

Algorithms should be numbered and include a short title. They are set off from the text with rules above and below the title and after the last line.

Algorithm 1 Weighted Tanimoto ELM.

TRAIN($\mathbf{XT}$)
  select randomly $W \subset \mathbf{X}$
  $N_{\mathbf{t}} \leftarrow |\{i : \mathbf{t}_i = \mathbf{t}\}|$ **for** $\mathbf{t} = -1, +1$
  $B_i \leftarrow \sqrt{\text{MAX}(N_{-1}, N_{+1})/N_{\mathbf{t}_i}}$ **for** $i = 1, ..., N$
  $\hat{\mathbf{H}} \leftarrow B \cdot (\mathbf{X}^T\mathbf{W})/(\not\Vdash\mathbf{X} + \not\Vdash\mathbf{W} - \mathbf{X}^T\mathbf{W})$
  $\beta \leftarrow \left(I/C + \hat{\mathbf{H}}^T\hat{\mathbf{H}}\right)^{-1} (\hat{\mathbf{H}}^T B \cdot \mathbf{T})$
  return $\mathbf{W}, \beta$

PREDICT($\mathbf{X}$)
  $\mathbf{H} \leftarrow (\mathbf{X}^T\mathbf{W})/(\not\Vdash\mathbf{X} + \not\Vdash\mathbf{W} - \mathbf{X}^T\mathbf{W})$
  return SIGN($\mathbf{H}\beta$)

Que sunt eum lam eos si dic to estist, culluptium quid qui nestrum nobis reiumquiatur minimus minctem. Ro moluptat fuga. Itatquiam ut laborpo rersped exceres vollandi repudaerem. Ulparci sunt, qui doluptaquis sumquia ndestiu sapient iorepella sunti veribus. Ro moluptat fuga. Itatquiam ut laborpo rersped exceres vollandi repudaerem.

IX. Mathematical Typography and Why It Matters

Typographical conventions for mathematical formulas have been developed to **provide uniformity and clarity of presentation across mathematical texts**. This enables the readers of those texts to both understand the author's ideas and to grasp new concepts quickly. While software such as LaTeX and MathType® can produce aesthetically pleasing math when used properly, it is also very easy to misuse the software, potentially resulting in incorrect math display.

IEEE aims to provide authors with the proper guidance on mathematical typesetting style and assist them in writing the best possible article. As such, IEEE has assembled a set of examples of good and bad mathematical typesetting [**?**], [**?**], [**?**], [**?**], [**?**].

Further examples can be found at http://journals.ieeeauthorcenter.ieee.org/wp-content/uploads/sites/7/IEEE-Math-Typesetting-Guide-for-LaTeX-Users.pdf

A. Display Equations

The simple display equation example shown below uses the "equation" environment. To number the equations, use the `\label` macro to create an identifier for the equation. LaTeX will automatically number the equation for you.

$$x = \sum_{i=0}^{n} 2iQ. \tag{2}$$

is coded as follows:

```
\begin{equation}
\label{deqn_ex1}
x = \sum_{i=0}^{n} 2{i} Q.
\end{equation}
```

To reference this equation in the text use the `\ref` macro. Please see (2)
is coded as follows:

```
Please see (\ref{deqn_ex1})
```

B. Equation Numbering

Consecutive Numbering: Equations within an article are numbered consecutively from the beginning of the article to the end, i.e., (1), (2), (3), (4), (5), etc. Do not use roman numerals or section numbers for equation numbering.
Appendix Equations: The continuation of consecutively numbered equations is best in the Appendix, but numbering as (A1), (A2), etc., is permissible.

Hyphens and Periods: Hyphens and periods should not be used in equation numbers, i.e., use (1a) rather than (1-a) and (2a) rather than (2.a) for subequations. This should be consistent throughout the article.

C. Multi-Line Equations and Alignment

Here we show several examples of multi-line equations and proper alignments.
A single equation that must break over multiple lines due to length with no specific alignment.

$$\begin{multline}\text{The first line of this example}\\ \text{The second line of this example}\\ \text{The third line of this example}\end{multline} \tag{3}$$

is coded as:

```
\begin{multline}
\text{The first line of this example}\\
\text{The second line of this example}\\
\text{The third line of this example}
\end{multline}
```

A single equation with multiple lines aligned at the = signs

$$a = c + d \tag{4}$$
$$b = e + f \tag{5}$$

is coded as:

```
\begin{align}
a &= c+d \\
b &= e+f
\end{align}
```

The `align` environment can align on multiple points as shown in the following example:

$$x = y \qquad X = Y \qquad a = bc \tag{6}$$
$$x' = y' \qquad X' = Y' \qquad a' = bz \tag{7}$$

is coded as:

```
\begin{align}
x &= y & X & =Y & a &=bc\\
x' &= y' & X' &=Y' &a' &=bz
\end{align}
```

D. Subnumbering

The amsmath package provides a `subequations` environment to facilitate subnumbering. An example:

$$f = g \tag{8a}$$
$$f' = g' \tag{8b}$$
$$\mathcal{L}f = \mathcal{L}g \tag{8c}$$

is coded as:

```
\begin{subequations}\label{eq:2}
\begin{align}
f&=g \label{eq:2A}\\
f' &=g' \label{eq:2B}\\
\mathcal{L}f &= \mathcal{L}g \label{eq:2c}
\end{align}
\end{subequations}
```

E. Matrices

There are several useful matrix environments that can save you some keystrokes. See the example coding below and the output.
A simple matrix:

$$\begin{matrix} 0 & 1 \\ 1 & 0 \end{matrix} \tag{9}$$

is coded as:

```
\begin{equation}
\begin{matrix}  0 &  1 \\
1 &  0 \end{matrix}
\end{equation}
```

A matrix with parenthesis

$$\begin{pmatrix} 0 & -i \\ i & 0 \end{pmatrix} \tag{10}$$

is coded as:

```
\begin{equation}
\begin{pmatrix} 0 & -i \\
 i &  0 \end{pmatrix}
\end{equation}
```

A matrix with square brackets

$$\begin{bmatrix} 0 & -1 \\ 1 & 0 \end{bmatrix} \tag{11}$$

is coded as:

```
\begin{equation}
\begin{bmatrix} 0 & -1 \\
1 &  0 \end{bmatrix}
\end{equation}
```

A matrix with curly braces

$$\begin{Bmatrix} 1 & 0 \\ 0 & -1 \end{Bmatrix} \tag{12}$$

is coded as:

```
\begin{equation}
\begin{Bmatrix} 1 &  0 \\
0 & -1 \end{Bmatrix}
\end{equation}
```

A matrix with single verticals

$$\begin{vmatrix} a & b \\ c & d \end{vmatrix} \tag{13}$$

is coded as:

```
\begin{equation}
\begin{vmatrix} a &  b \\
c &  d \end{vmatrix}
\end{equation}
```

A matrix with double verticals

$$\begin{Vmatrix} i & 0 \\ 0 & -i \end{Vmatrix} \tag{14}$$

is coded as:

```
\begin{equation}
\begin{Vmatrix} i &  0 \\
0 & -i \end{Vmatrix}
\end{equation}
```

F. Arrays

The `array` environment allows you some options for matrix-like equations. You will have to manually key the fences, but there are other options for alignment of the columns and for setting horizontal and vertical rules. The argument to `array` controls alignment and placement of vertical rules.

A simple array

$$\left(\begin{array}{cccc} a+b+c & uv & x-y & 27 \\ a+b & u+v & z & 134 \end{array} \right) \tag{15}$$

is coded as:

```
\begin{equation}
\left(
\begin{array}{cccc}
a+b+c & uv & x-y & 27\\
a+b & u+v & z & 134
\end{array} \right)
\end{equation}
```

A slight variation on this to better align the numbers in the last column

$$\left(\begin{array}{cccc} a+b+c & uv & x-y & 27 \\ a+b & u+v & z & 134 \end{array} \right) \tag{16}$$

is coded as:

```
\begin{equation}
\left(
\begin{array}{cccr}
a+b+c & uv & x-y & 27\\
a+b & u+v & z & 134
\end{array} \right)
\end{equation}
```

An array with vertical and horizontal rules

$$\left(\begin{array}{c|c|c|r} a+b+c & uv & x-y & 27 \\ \hline a+b & u+v & z & 134 \end{array} \right) \tag{17}$$

is coded as:

```
\begin{equation}
\left(
\begin{array}{c|c|c|r}
a+b+c & uv & x-y & 27\\
a+b & u+v & z & 134
\end{array} \right)
\end{equation}
```

Note the argument now has the pipe "|" included to indicate the placement of the vertical rules.

G. Cases Structures

Many times cases can be miscoded using the wrong environment, i.e., `array`. Using the `cases` environment will save keystrokes (from not having to type the `\left\lbrace`) and automatically provide the correct column alignment.

$$z_m(t) = \begin{cases} 1, & \text{if } \beta_m(t) \\ 0, & \text{otherwise.} \end{cases}$$

is coded as follows:

```
\begin{equation*}
{z_m(t)} =
\begin{cases}
1,&{\text{if}}\ {\beta }_m(t),\\
{0,}&{\text{otherwise.}}
\end{cases}
\end{equation*}
```

Note that the "&" is used to mark the tabular alignment. This is important to get proper column alignment. Do not use `\quad` or other fixed spaces to try and align the columns. Also, note

the use of the \text macro for text elements such as "if" and "otherwise."

H. Function Formatting in Equations

Often, there is an easy way to properly format most common functions. Use of the \ in front of the function name will in most cases, provide the correct formatting. When this does not work, the following example provides a solution using the \text macro:

$$d_R^{KM} = \arg\min_{d_l^{KM}} \{d_1^{KM}, \ldots, d_6^{KM}\}.$$

is coded as follows:

```
\begin{equation*}
 d_{R}^{KM} = \underset {d_{l}^{KM}}
 {\text{arg min}} \{ d_{1}^{KM},
 \ldots,d_{6}^{KM}\}.
\end{equation*}
```

I. Text Acronyms Inside Equations

This example shows where the acronym "MSE" is coded using \text{} to match how it appears in the text.

$$\text{MSE} = \frac{1}{n}\sum_{i=1}^{n}(Y_i - \hat{Y}_i)^2$$

```
\begin{equation*}
 \text{MSE} = \frac {1}{n}\sum _{i=1}^{n}
(Y_{i} - \hat {Y_{i}})^{2}
\end{equation*}
```

X. Conclusion

The conclusion goes here.

Acknowledgments

The authors would also thank people helping during the measurement campaigns. M.Sc. Alessandro Benegiamo, M.Sc. Veronica Vila, Eva Martín and M.Sc. Eduardo "Lalo" Caballero were part of the team that allow this work to achieve excellence.

References

[1] K. Persaud, "Medical applications of odor-sensing devices," *International Journal of Lower Extremity Wounds*, vol. 4, no. 1, pp. 50–56, 2005.

[2] L. Capelli, S. Sironi, and R. Del Rosso, "Electronic noses for environmental monitoring applications," *Sensors (Basel)*, vol. 14, no. 11, pp. 19 979–2007, 2014.

[3] V. Di Lecce, D. Petruzzelli, C. Guaragnella, A. Cardellicchio, G. Dentamaro, A. Quarto, D. Soldo, and R. Dario, "Real-time monitoring system for urban wastewater," in *2017 IEEE Workshop on Environmental, Energy, and Structural Monitoring Systems (EESMS)*. IEEE, 2017, pp. 1–5.

[4] A. Blanco-Rodriguez, V. Camara, F. Campo, L. Becheran, A. Duran, V. Vieira, H. de Melo, and A. Garcia-Ramirez, "Development of an electronic nose to characterize odours emitted from different stages in a wastewater treatment plant," *Water Research*, vol. 134, pp. 92–100, 2018.

[5] F. Cangialosi, G. Intini, and D. Colucci, "On line monitoring of odour nuisance at a sanitary landfill for non-hazardous waste," *Chem. Eng. Trans*, vol. 68, pp. 127–132, 2018.

[6] M. Daelman, E. van Voorthuizen, U. van Dongen, E. Volcke, and M. van Loosdrecht, "Methane emission during municipal wastewater treatment," *Water Research*, vol. 46, no. 11, pp. 3657–3670, 2012.

[7] S. Prudenza, C. Bax, and L. Capelli, "Implementation of an electronic nose for real-time identification of odour emission peaks at a wastewater treatment plant," *Heliyon*, vol. 9, no. 10, 2023.

[8] D. Cipriano and L. Capelli, "Evolution of electronic noses from research objects to engineered environmental odour monitoring systems: A review of standardization approaches," *Biosensors*, vol. 9, no. 2, p. 75, 2019.

[9] S. Deshmukh, R. Bandyopadhyay, N. Bhattacharyya, R. Pandey, and A. Jana, "Application of electronic nose for industrial odors and gaseous emissions measurement and monitoring–an overview," *Talanta*, vol. 144, pp. 329–340, 2015.

[10] C. Ratti, C. Bax, B. Lotesoriere, and L. Capelli, "Real-time monitoring of odour emissions at the fenceline of a waste treatment plant by instrumental odour monitoring systems: Focus on training methods," *Sensors*, vol. 24, no. 11, p. 3506, 2024.

[11] T. Pobkrut, T. Eamsa-Ard, and T. Kerdcharoen, "Sensor drone for aerial odor mapping for agriculture and security services," in *2016 13th International Conference on Electrical Engineering/Electronics, Computer, Telecommunications and Information Technology (ECTI-CON)*. IEEE, 2016, pp. 1–5.

[12] J. Burgues, M. Deseada Esclapez, S. Donate, and S. Marco, "Rhinos: a lightweight portable electronic nose for real-time odor quantification in wastewater treatment plants," *iScience*, vol. 24, no. 12, 2021.

[13] J. Burgues, S. Donate, M. Esclapez, L. Sauco, and S. Marco, "Characterization of odour emissions in a wastewater treatment plant using a drone-based chemical sensor system," *Science of the Total Environment*, vol. 846, p. 15729, 2022.

[14] G. Tassielli, L. Cananà, and M. Spalatro, "Detection of methane leaks via a drone-based system for sustainable landfills and oil and gas facilities: Effect of different variables on the background-noise measurement," *Sustainability*, vol. 16, no. 17, p. 7748, 2024.

[15] M. Yandouzi, M. Grari, M. Berrahal, I. Idrissi, O. Moussaoui, M. Azizi, K. Ghoumid, and A. Elmiad, "Investigation of combining deep learning object recognition with drones for forest fire detection and monitoring," *International Journal of Advanced Computer Science and Applications*, vol. 14, no. 3, 2023.

[16] J. Burgués and S. Marco, "Drone-based monitoring of environmental gases," in *Air Quality Networks, Environmental Informatics and Modeling*, S. De Vito *et al.*, Eds. Springer Nature Switzerland AG, 2023, pp. 115–136.

[17] J. Burgués, L. Valdez, and S. Marco, "High-bandwidth e-nose for rapid tracking of turbulent plumes," in *2019 IEEE International Symposium on Olfaction and Electronic Nose (ISOEN)*. Fukuoka, Japan: IEEE, 2019, pp. 1–3.

[18] F. Cangialosi, E. Bruno, and A. Fornaro, "Integrating citizen science and machine learning algorithms for the recognition of odour classes nearby a wastewater treatment plant," *Chemical Engineering Transactions*, vol. 95, pp. 25–30, Oct 2022.

[19] A. Benegiamo, J. Burgués, J. Alonso-Valdesueiro, B. Lotesoriere, L. Terrén, L. Sauco, M. Esclapez, S. Doñate, A. Gutiérrez-Gálvez, and S. Marco, "Optimization of a drone-based system for instrumental odor monitoring using feature selection," *Proceedings*, vol. 97, p. 109, 2024.

[20] J. Alonso-Valdesueiro, S. Marco, and A. Gutierrez-Galvez, "Drone-nose: drone-embedded measurement platform for odour monitoring," in *IEEE International Symposium on Olfaction and Electronic Nose, ISOEN 2024, Grapevine, TX, USA, May 12-15, 2024*. IEEE, 2024, pp. 1–3. [Online]. Available: https://doi.org/10.1109/ISOEN61239.2024.10556083

XI. Biographies

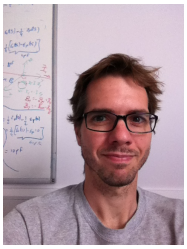

Javier Alonso-Valdesueiro was born in Madrid, Spain, in 1980. He received his Telecommunications Engineering degree from the University of Alcalá, Madrid, in 2006, and his Ph.D. degree from the Polytechnic University of Catalonia, Barcelona, in 2011. From 2012 to 2020, he worked on developing electronic instrumentation for NMR experiments, initially at the C.E.A Center in France, followed by the University of Southampton in the UK, and later as a Marie Skłodowska-Curie Fellow at the University of the Basque Country (UPV/EHU). Over the past four years, he has advanced his career as an RF and instrumentation engineer in both private companies and public research centers, including TECNALIA Innovation Foundation and the Institute of Biomedical Engineering of Catalonia. Recently, he has been appointed as Assistant Professor in the Department of Electronic and Biomedical Engineering at the University of Barcelona.